Astron. Astrophys. 322, 329–339 (1997)

ASTRONOMY
AND
ASTROPHYSICS

Temporal evolution of resonant absorption in coronal loops

Excitation by footpoint motions normal to the magnetic surfaces

W.J. Tirry[⋆], **David Berghmans**[*], **and Marcel Goossens**

Centre for Plasma Astrophysics, K.U. Leuven, Celestijnenlaan 200 B, B-3001 Heverlee, Belgium

Received 3 October 1996 / Accepted 21 November 1996

Abstract. In this paper we study the temporal evolution of linear MHD waves excited by footpoint motions using an ideal, pressureless slab model for coronal loops. We choose the footpoint motions to be polarised normal to the magnetic flux surfaces such that only fast waves are driven directly, including the so-called quasi-modes. We have derived a formal analytical solution as a superposition of eigenmodes describing the system as a function of time. The corresponding eigenvalue problem is solved numerically. This enables us to study the influence of the characteristics of the footpoint motion on the excitation of the quasi-modes. On the magnetic flux surface where the frequency of these quasi-modes equals the local Alfvén frequency, wave energy is transferred from the quasi-modes towards Alfvén waves. We investigate the time evolution of this process in which small scale dissipative features are generated which can be relevant in the context of coronal heating.

Special attention is given to the question whether this generation of small scale dissipative features takes place on time scales shorter than typical life times of coronal loops. Expressing the dissipation time scale as function of the length scale corresponding to the resonances, an estimate for the time when dissipation becomes important and when our ideal MHD simulation stops to be valid, can be derived. For typical dissipation coefficients and length scales, dissipation becomes important in the resonance layer in a time comparable to the life time of coronal loops.

Key words: MHD – Sun: corona – Sun: magnetic fields-waves – methods: analytical

1. Introduction

The solar corona consists of highly inhomogeneous plasma with a temperature of roughly 3×10^6 K. This temperature is a few orders higher than the underlying photospheric temperature, indicating the presence of heating mechanisms. Since Skylab it is known that the largest contribution to the X-ray emission and to the heating of the solar corona comes from loop like structures in the solar atmosphere. These magnetic loops are viewed as the basic building blocks of the solar corona. The high conductivity and the relatively high mass density of the photospheric plasma provide an effective photospheric anchoring of the magnetic field lines. These photospheric footpoints of the magnetic field lines are forced to follow the convective motions. If these footpoint motions are slow (in comparison with the Alfvénic transit time along the loop), the coronal flux tubes are twisted and braided, which builds up magnetic stresses and leads to the formation of small length scale by the creation of field discontinuities (Parker 1972) or by cascade of magnetic energy to very small length scales (Van Ballegooijen 1985). These mechanisms to generate small length scales, and hence heating, are usually classified as DC heating mechanisms (Zirker 1993).

In contrast, footpoint motions which are 'fast' in comparison with the Alfvénic transit time, generate magnetosonic waves and Alfvén waves. Due to the steep density gradients at the photospheric edges these MHD waves reflect back and forth along the length of the loop. The loop is then expected to act as a leaking, resonant cavity for MHD waves (Hollweg 1984). Some observational evidence of MHD waves propagating in coronal loops has indeed been reported. The UV spectrum suggests nonthermal velocities of 10-20 km/s (Cheng, Doschek & Feldman 1979). Recent studies of soft X-ray lines from the XRP indicate nonthermal motions of 30-40 km/s above active regions (Saba & Strong 1991).

An important property of MHD waves in an inhomogeneous plasma is that a global wave motion can be in resonance with local oscillations of a specific magnetic surface. The resonance condition is that the frequency of the global motion is equal to either the local Alfvén or the local cusp frequency of the magnetic surface. In this way energy is transferred from the large scale motion to oscillations which are highly localised to the neighbourhood of the Alfvén or cusp singular surface. In dissipative MHD this behaviour is mathematically recovered as eigenmodes which are exponentially damped in time. Due to their global character (oscillating with the same frequency throughout the plasma) these modes are called 'global modes'. For ideal

Send offprint requests to: M. Goossens

⋆ Research Assistant of the Belgian National Fund for Scientific Research

MHD such a damped oscillation cannot be an eigenmode of the system, and for this reason they are often called 'quasi-modes' (see Tirry & Goossens 1996 and references therein).

A lot of work, both analytically and numerically, was done on sideways excitation where a wave impinges laterally on the loop (Poedts et al. 1989; Poedts & Kerner 1992; Steinolfson & Davila 1993; Ofman & Davila 1995, 1996; Wright & Rickard 1995). This problem is mathematically easier than the case of footpoint excitation since the impinging wave can be included as a source term or boundary condition for the radial equation without having to solve the longitudinal equation explicitly. Such an impinging MHD wave must necessarily be a fast wave since Alfvén waves cannot transport energy perpendicular to the magnetic field and slow waves are negligible in the corona due to the low gas pressure. When a loop is perturbed by a broad band spectrum on its side surface, it will respond at a discrete set of frequencies of fast waves which may resonantly excite Alfvén waves in turn. Hence the plasma-driver coupling was found to be very efficient due to the effect of the present global modes (Wright & Rickard 1995).

However it is important to see that sideways excitation by an externally impinging fast wave can only yield a minor contribution to the heating of a coronal loop by resonant absorption. Due to the enhanced density the interior Alfvén speed must be smaller than the exterior Alfvén speed. Therefore only fast waves which are exponentially decaying on their way to the loop can resonantly excite Alfvén waves inside the loop. This suggest that fast waves originating from within the loop must be the prime contribution. Such fast wave can be excited by e.g. a reconnection event inside the loop or by the photospheric motions of the footpoints of the magnetic field lines.

The photospheric excitation of resonant waves has been subject to criticism. Here the important question arises whether the photosphere in fact offers sufficient power at the right frequencies. Parker (1992) argues that the involved time scale, corresponding to the turn-over-time of the individual granules, is much too long. But as pointed out by Goedbloed (1994) a mechanism, similar to the stick slip mechanism that makes it possible for the violinist to excite frequencies of 200 Hz to more than 2000 Hz by a several orders of magnitude lower periodic motion of the bow, might overcome this problem. However such an equivalent mechanism has not been found yet.
As discussed in the overview on heating mechanisms by Zirker (1993), the observations available so far are not sufficiently detailed to either exclude or confirm the generation of large enough wave fluxes in the photosphere. Very promising in this context are the recent observations by Ulrich (1996) who reported magnetic oscillations in the photosphere which were identified as outgoing Alfvén waves with substantial power at low frequencies.

Furthermore the theoretical investigation on footpoint excitation of MHD waves has only recently been reported. More precisely we feel that the 'missing link' in wave heating scenarios by resonant absorption is the question of how resonant Alfvén waves can be indirectly driven by footpoint motions through coupling with 'global modes'. This problem involves the explicit solution of the wave-dynamics not only in the radial direction, but also in the longitudinal direction in order to include the appropiate boundary conditions at the loop's feet. Moreover it is advisable to study the initial value problem, since an asymptotic state may well be inattainable (Berghmans & De Bruyne 1995). As a consequence the photospheric excitation of global modes and their subsequent coupling to resonant Alfvén waves turns out to be a difficult mathematical problem.

Recently Goedbloed & Halberstadt (1993) showed that line-tying completely changes the character of the basic MHD waves occuring in a coronal loop as compared to those in a periodic system. MHD waves of mixed nature occur: the waves consist of large amplitude Alfvén components in the corona and fast components with a small but rapidly varying amplitude in the photospheric boundary layers. Halberstadt & Goedbloed (1994) noticed that a new line-tied continuum appears with the most important feature that it does not depend on the poloidal magnetic field and mode number. However in the present paper this coupling is absent because of the choice of a straight magnetic field as described in the physical model in Sect. 2.

Due to the intrinsic difficulty of the footpoint driven problem, authors have often assumed the torsional wave-number to be zero in order to avoid complications with the coupling of quasi-modes and Alfvén waves (Heyvaerts & Priest 1983; Berghmans & De Bruyne 1995; Berghmans, De Bruyne and Goossens 1996; Poedts & Boyton 1996; Ruderman et al. 1996). A remarkable exception to this restriction has been the work of Halberstadt & Goedbloed (1995a,b). They calculated the stationary state solutions in the case of footpoint excitation of Alfvén waves and in the case of an external surface excitation source at the ends of the loops. Their results leave little doubt: the coupling of the global wave to the localized Alfvén wave strongly increases the dissipation rate in the vicinity of the eigenfrequency.

None of the above mentioned papers really answered the question whether the development of resonant layers and the involved phase-mixing are effective in producing the necessary dissipative small scales on acceptable time scales, consistent with the dissipative coefficients corresponding to the coronal conditions and with the observed length scales of the coronal loops. The maximal values of the Reynolds numbers in the numerical simulations are limited by the resolution and numerical dissipation and are small compared to the solar values. Poedts, Beliën & Goedbloed (1994) showed that the resonances (by sideways excitation) in coronal loops have bad quality (the quality Q of a resonance is defined as the ratio of the total energy contained in the system to the dissipation per driving cycle). This means a lot of Ohmic heating per driving cycle compared to the total energy stored in the loop. As a consequence, they conclude that the time scales of the heating process can be relatively short and resonant absorption turns out to be a viable candidate for the heating of the magnetic loops observed in the solar corona.

The main topic of the present paper is a time-dependent study of resonant excitation of Alfvén waves in coronal loops by coupling to quasi-modes which are generated by photospheric

motions of the footpoints of the magnetic fieldlines. We start in the next section by describing the slab model used for a coronal loop. Since photospheric excitation involves also a velocity component in the radial direction, we focus on excitation of linear MHD waves by radially polarised footpoint motions. The relevant MHD equations and the underlying assumptions are discussed. Inspired by Berghmans, De Bruyne & Goossens (1996) we derive a formal analytic expression for the temporal evolution of the excited MHD waves as a superposition of eigenmodes (Sect. 3a). To solve the corresponding eigenvalue problem we resort to the method described by Mann, Wright & Cally (1995). This approximative method, based on the truncation of a Fourier series, assures that the structure of the waves is fully resolved at any time (Sect. 3b). The combination of the analytical findings and the numerical work yields an expression for the linear wave amplitudes at any point in 3D, and at any time as a result of the ongoing footpoint driving. In Sect. 4 we use this semi analytical/numerical expression to illustrate the effect of the present global modes on the excitation of resonant Alfvén waves with an instructive example. By following the dissipation time scale corresponding to the length scale of the resonance as function of the physical time, the outcome of our linear ideal MHD simulations is that dissipation becomes important in the resonance layer in a time comparable to the life time of coronal loops (Sect. 5). Finally Sect. 6 gives a summary and discussion.

2. Physical model

A coronal loop is modelled as a static, straight, gravitationless plasma slab with thickness a, obeying the standard set of ideal MHD equations. In the Cartesian coordinate system which we use, the x-coordinate corresponds to the radial direction, y-coordinate to the (ignorable) azimuthal coordinate and the z-coordinate represents the direction along the loop.

At $z = 0$ we impose a given footpoint motion whereas at $z = L$ we assume the loop to be line-tied. This can be done without any loss of generality because of the principle of superposition for solutions of linear equations. The boundary planes model the sharp transition from the corona to the photosphere (i.e. transition region, chromosphere and photosphere). We shall refer to these boundary planes as being the 'photospheric edges' of the loop and we implicitly assume that a disturbance initiated in the photosphere indeed reaches the corona. In the radial direction we assume for mathematical tractability rigid wall conditions at $x = 0$ and $x = a$. We think of $x = 0$ being the inside of the loop and $x = a$ being the exterior coronal environment. Later we will return to the issue of the physical consequences of modelling a coronal loop as a closed box instead of an open system.

The plasma is permeated by a uniform magnetic field ($\mathbf{B_0} = B_0\mathbf{e_z}$) and has a uniform pressure p_0 which we neglect in comparison with the magnetic pressure. Inhomogeneity of the plasma is introduced by a continuously varying density

$$\rho_0(x) = \rho_A + \rho_B \cos(\frac{\pi}{a}x) \quad \text{with} \quad \rho_B < \rho_A, \tag{1}$$

which models the higher density inside the loop.

Since we did not take into account a z-dependence of the density, our analysis is to be applied to coronal loops with their apex lower than one scale height.

The plasma is being shaken by small-amplitudes perturbations at the footpoints of the magnetic field lines on the $z = 0$ plane. As long as non-linear and non-ideal effects are negligible we can follow the temporal evolution of the excited MHD waves inside the loop by solving the linear ideal MHD equations. The linear ideal MHD equations reduce for a pressureless plasma to

$$\{\frac{1}{v_A^2}\frac{\partial^2}{\partial t^2} - \frac{\partial^2}{\partial z^2} - \frac{\partial^2}{\partial x^2}\}\xi_x = \frac{\partial^2 \xi_y}{\partial y \partial x}, \tag{2}$$

$$\{\frac{1}{v_A^2}\frac{\partial^2}{\partial t^2} - \frac{\partial^2}{\partial z^2} - \frac{\partial^2}{\partial y^2}\}\xi_y = \frac{\partial^2 \xi_x}{\partial y \partial x}. \tag{3}$$

where ξ is the Lagrangian displacement and the Alfvén speed v_A is given by

$$v_A(x) = \sqrt{\frac{B_0^2}{\mu\rho_0(x)}}.$$

This coupled system of partial differential equations in ξ_x and ξ_y describes the coupled fast-Alfvén waves. Slow waves are absent ($\xi_z = 0$) because the plasma pressure was neglected.

Since the equilibrium quantities are constant in the y-coordinate which runs over an infinite domain, we can Fourier analyse with respect to y. For the Fourier component corresponding to wave number k_y, the time evolution and the spatial variation in x and z are described by

$$\{\frac{1}{v_A^2}\frac{\partial^2}{\partial t^2} - \frac{\partial^2}{\partial z^2} - \frac{\partial^2}{\partial x^2}\}\xi_x = ik_y\frac{\partial \xi_y}{\partial x}, \tag{4}$$

$$\{\frac{1}{v_A^2}\frac{\partial^2}{\partial t^2} - \frac{\partial^2}{\partial z^2} + k_y^2\}\xi_y = ik_y\frac{\partial \xi_x}{\partial x}. \tag{5}$$

Berghmans & De Bruyne (1995) and Berghmans, De Bruyne & Goossens (1996) simplified these equations by focussing on y-independent motions. In this case the fast and Alfvén waves are decoupled. Berghmans & De Bruyne give a fully analytical treatment of the time evolution of torsional Alfvén waves (corresponding to the ξ_y component as described by Eq. (5)). Berghmans, De Bruyne & Goossens extended the analysis to the sausage waves (corresponding to the ξ_x component as described by Eq. (4)) which are excited by radially polarised footpoint motions.

Following closely their analysis we solve in the present paper the coupled Eqs. (4) and (5). Since the photospheric excitation involves also a velocity component in the radial direction, we focus on the excitation by radially polarised footpoint motions. Note that in this way Alfvén waves are not directly excited.

3. Mathematical approach

In this section we derive a formal analytical solution of the coupled equations (4) and (5) which describes the temporal evolution of linear MHD waves excited by radially polarised

footpoint motions. The analysis is based on the papers by Mann, Wright & Cally (1995) and Berghmans, De Bruyne & Goossens (1996). Mann, Wright & Cally investigated the coupling of magnetospheric cavity modes to field line resonances. The matrix eigenvalue method that they used to follow the irreversible coupling between the fast magnetospheric cavity modes and the resonant Alfvén waves forms the basis of the numerical side of our approach. The second paper, by Berghmans, De Bruyne & Goossens, who considered the uncoupled equation for the fast waves, inspired the analytical approach which takes in a handy way the radially polarised footpoint motions into account.

3.1. Formal analytical solution

We represent the radially polarised footpoint motions by inhomogeneous boundary conditions for Eqs. (4) and (5) at the $z = 0$ and the $z = L$ boundary planes.

$$\begin{aligned}
\xi_x(x, y, z = 0, t) &= R(x)T(t)e^{ik_y y}, \\
\xi_x(x, y, z = L, t) &= 0, \\
\xi_y(x, y, z = 0, t) &= 0, \\
\xi_y(x, y, z = L, t) &= 0.
\end{aligned}$$

We have assumed for mathematical simplicity that the dependencies on x and t of the footpoint motions are separable. In order to avoid complications with initial conditions we assume in addition that

$$\begin{aligned}
\xi_x(x, y, z, t = 0) &= \frac{\partial \xi_x(x, y, z, t = 0)}{\partial t} = 0, \\
\xi_y(x, y, z, t = 0) &= \frac{\partial \xi_y(x, y, z, t = 0)}{\partial t} = 0,
\end{aligned}$$

which leads to

$$T(t = 0) = \frac{\partial T(t = 0)}{\partial t} = 0. \tag{6}$$

Apart from these restrictions the functions $R(x)$ and $T(t)$ can be chosen completely arbitrarily. With the aid of the function

$$\chi(x, y, z, t) = \xi_x(x, y, z, t) - (1 - \frac{z}{L})R(x)T(t)e^{ik_y y},$$

we include the footpoint motions as a driving term in the equations, while the boundary conditions become homogeneous

$$\begin{aligned}
\{\frac{1}{v_A^2}\frac{\partial^2}{\partial t^2} &- \frac{\partial^2}{\partial z^2} - \frac{\partial^2}{\partial x^2}\}\chi = \\
&ik_y \frac{\partial \xi_y}{\partial x} + (1 - \frac{z}{L})\{\frac{\partial^2}{\partial x^2} - \frac{1}{v_A^2}\frac{\partial^2}{\partial t^2}\}R(x)T(t),
\end{aligned} \tag{7}$$

$$\begin{aligned}
\{\frac{1}{v_A^2}\frac{\partial^2}{\partial t^2} &- \frac{\partial^2}{\partial z^2} + k_y^2\}\xi_y = \\
&ik_y \frac{\partial \xi_x}{\partial x} + (1 - \frac{z}{L})ik_y \frac{\partial R}{\partial x}T(t),
\end{aligned} \tag{8}$$

and

$$\chi(z = 0) = 0 = \chi(z = L), \quad \xi_y(z = 0) = 0 = \xi_y(z = L).$$

These homogeneous boundary conditions for χ and ξ_y now allow for the following sine-expansions

$$\begin{aligned}
\chi(x, y, z, t) &= \frac{2}{L}\sum_{n=1}^{\infty} X^{(n)}(x, y, t)\sin(\frac{n\pi}{L}z), \\
i\xi_y(x, y, z, t) &= \frac{2}{L}\sum_{n=1}^{\infty} Y^{(n)}(x, y, t)\sin(\frac{n\pi}{L}z).
\end{aligned}$$

Expanding the function $(1 - \frac{z}{L})$ in Eqs. (7) and (8) in a series of sines results in

$$1 - \frac{z}{L} = \frac{2}{L}\sum_{n=1}^{\infty}\frac{L}{n\pi}\sin(\frac{n\pi}{L}z) \quad \text{for } z \in]0, L], \tag{9}$$

where the righthandside is convergent for all values of z but $z = 0$. This poses no difficulties since in what follows we only look for a weak solution. With the use of the sine-transforms the coupled partial differential Eqs. (7) and (8) are replaced by an infinite set of coupled ODE for $X^{(n)}$ and $Y^{(n)}$. There is no coupling between different n-modes.

$$\begin{aligned}
\{\frac{1}{v_A^2}\frac{\partial^2}{\partial t^2} &+ (\frac{n\pi}{L})^2 - \frac{\partial^2}{\partial x^2}\}X^{(n)} \\
&= k_y \frac{\partial Y^{(n)}}{\partial x} + \frac{L}{n\pi}\{\frac{\partial^2}{\partial x^2} - \frac{1}{v_A^2}\frac{\partial^2}{\partial t^2}\}R(x)T(t)
\end{aligned} \tag{10}$$

$$\begin{aligned}
\{\frac{1}{v_A^2}\frac{\partial^2}{\partial t^2} &+ (\frac{n\pi}{L})^2 + k_y^2\}Y^{(n)} \\
&= -k_y \frac{\partial X^{(n)}}{\partial x} - \frac{L}{n\pi}k_y \frac{\partial R}{\partial x}T(t)
\end{aligned} \tag{11}$$

Since we are interested in the time evolution, a logical next step in the mathematical analysis is the Laplace transform technique

$$\begin{aligned}
\hat{Q}(\omega) &= \int_0^{\infty} Q(t)e^{i\omega t}dt, \\
Q(t) &= \frac{1}{2\pi}\int_C \hat{Q}(\omega)e^{-i\omega t}d\omega,
\end{aligned}$$

where C is the Bromwich integration path running parallel to the real axis of the ω-plane above all singularities of $\hat{Q}(\omega)$. Applying this transformation for Eqs. (10) and (11) yields

$$\{A[n] - \omega^2\}\begin{bmatrix}\hat{X}^{(n)} \\ \hat{Y}^{(n)}\end{bmatrix} = B[n] \tag{12}$$

where

$$\begin{aligned}
A[n] &= v_A^2\begin{bmatrix}(\frac{n\pi}{L})^2 - \frac{\partial^2}{\partial x^2} & -k_y\frac{\partial}{\partial x} \\ k_y\frac{\partial}{\partial x} & (\frac{n\pi}{L})^2 + k_y^2\end{bmatrix}, \\
B[n] &= \frac{L}{n\pi}v_A^2\hat{T}\begin{bmatrix}\frac{\partial^2 R}{\partial x^2} + \frac{\omega^2}{v_A^2}R \\ -k_y\frac{\partial R}{\partial x}\end{bmatrix}.
\end{aligned}$$

The Eq. (12) can be solved by inverting the operator $A[n]-\omega^2$. Formally this is not a problem, because $A[n]$ corresponds to the ideal MHD force operator which is Hermitian with respect to the following scalar product

$$< \xi_1|\xi_2 >= \int_0^a \xi_1\xi_2^*\rho dx. \tag{13}$$

It is well known that the eigenfunctions form a complete set so that the solution to Eq. (12) can be written as a spectral representation:

$$\begin{bmatrix}\hat{X}^{(n)}\\ \hat{Y}^{(n)}\end{bmatrix} = \sum_k \frac{1}{\omega_k^2-\omega^2}|\psi_k^n >< \psi_k^n|B[n] > + \int \frac{1}{\sigma^2-\omega^2}|\psi_\sigma^n >< \psi_\sigma^n|B[n] > d\sigma, \tag{14}$$

with orthonormal discrete and continuum eigenfunctions

$$\begin{aligned} < \psi_k^n|\psi_l^n > &= \delta_{kl},\\ < \psi_\sigma^n|\psi_\gamma^n > &= \delta(\sigma-\gamma),\\ < \psi_k^n|\psi_\sigma^n > &= 0. \end{aligned}$$

3.2. The eigenvalue problem

In this subsection we tackle the eigenvalue problem

$$A[n]|\psi_\omega^n >= \omega^2|\psi_\omega^n >,$$

with boundary conditions

$$|\psi_\omega^n >_1 |_{x=0} = 0 = |\psi_\omega^n >_1 |_{x=1},$$

where $|\psi_\omega^n >_1$ is the first component of $|\psi_\omega^n >$. Note that the length is nondimensionalized with respect to a. To satisfy these boundary conditions, we expand $|\psi_\omega^n >_1$ (corresponding to ξ_x) as a Fourier sine series. The form of Eq. (12) then suggest that $|\psi_\omega^n >_2$ (corresponding to ξ_y) can be expanded in a cosine series :

$$\begin{aligned} |\psi_\omega^n >_1 (x) &= \sum_{m=1}^{\infty} \alpha_m^n \sin(m\pi x),\\ |\psi_\omega^n >_2 (x) &= \frac{1}{2}\beta_0^n + \sum_{m=1}^{\infty} \beta_m^n \cos(m\pi x). \end{aligned}$$

Cally (1991) noted that with the given density profile (1) the eigenvalue problem can be written as a single generalised matrix eigenvalue problem. This eigenvalue problem is solved by truncating the expansions to $m \leq N$: the $2N+1$ eigenvalues and the coefficients α_m^n and β_m^n of the corresponding eigenvectors of the resulting *finite* matrix eigenvalue problem are easily found with the help of the NAGroutines F02FHF and F02SDF. With these eigenvalues and eigenvectors we can reconstitute the spectral representation (14). We refer to Appendix A of Mann, Wright & Cally (1995) for a description of the technical details of this method.

This method has several advantages over more standard finite differencing schemes. Notably, by taking a sufficiently large number of Fourier modes, and following the propagation towards finer scales through resonant absorption and phase mixing, we can ensure that at any time the structure of the waves is being fully resolved. In addition, we can compute the resolved wave structures at any time by calculating the Fourier summation. This results in a considerable CPU-time saving in comparison with usual finite difference approaches, whereby the disturbance must be calculated at every previous timestep.

It has been checked that for the finite matrix eigenvalue problem the eigenfunctions remain orthogonal with respect to the scalar product (13). As long as the finest scale in the x-direction of the MHD waves in the time evolution can be represented by $\sin(N\pi x)$ or $\cos(N\pi x)$, the spectral representation of $\hat{X}^{(n)}$ and $\hat{Y}^{(n)}$ can be adequately approximated by the sum over the discrete set of eigenfunctions of the finite generalised eigenvalue problem.

$$\hat{X}^{(n)}(x,\omega) = \sum_{m=1}^{N}\sum_{k=1}^{2N+1} \frac{\alpha_{mk}^n}{\omega_k^2-\omega^2} < \psi_k^n|B[n] > \sin(m\pi x), \tag{15}$$

$$\hat{Y}^{(n)}(x,\omega) = \frac{1}{2}\sum_{k=1}^{2N+1} \frac{\beta_{0k}^n}{\omega_k^2-\omega^2} < \psi_k^n|B[n] > + \sum_{m=1}^{N}\sum_{k=1}^{2N+1} \frac{\beta_{mk}^n}{\omega_k^2-\omega^2} < \psi_k^n|B[n] > \cos(m\pi x), \tag{16}$$

or in matrix notation

$$\begin{bmatrix}\hat{X}^{(n)}\\ \hat{Y}^{(n)}\end{bmatrix} = \sum_{k=1}^{2N+1} \frac{1}{\omega_k^2-\omega^2}|\psi_k^n >< \psi_k^n|B[n] > . \tag{17}$$

3.3. Inversion of transformations

We now want to invert the Laplace transform with respect to time and the sine transform with respect to z. For footpoint motions that can be described by a separable functions $R(x)T(t)$ the scalar product of the eigenfunctions and $B[n]$ reduces to

$$< \psi_k^n|B[n] >= \hat{T}(\omega)\{\frac{L}{n\pi}(\omega^2-\omega_k^2) < \psi_k^n|R(x) > + \frac{n\pi}{L}R_k^n\}, \tag{18}$$

where R_k^n is the scalar product without weightfunction of $R(x)$ and $|\psi_k^n >$

$$R_k^n = \int_0^1 R(x)|\psi_k^n(x) > dx.$$

Equation (17) can then be written as

$$\begin{bmatrix}\hat{X}^{(n)}\\ \hat{Y}^{(n)}\end{bmatrix} = -\frac{L}{n\pi}R(x)\hat{T}(\omega) + \frac{n\pi}{L}\hat{T}(\omega)\sum_{k=1}^{2N+1}\frac{R_k^n}{\omega_k^n-\omega^2}|\psi_k^n > . \tag{19}$$

The Laplace-inversion of the first term of expression (19) is straightforward

$$-\frac{L}{n\pi}\hat{T}(\omega)R(x) \rightarrow -\frac{L}{n\pi}T(t)R(x)$$

To perform the Laplace inversion of the second term of expression (19) we first note that the complete ω-dependence is contained in the factor

$$\frac{\hat{T}(\omega)}{\omega_k^2-\omega^2}.$$

Secondly one should remember the well known inversions

$$\frac{1}{\omega_k^2-\omega^2} \rightarrow \frac{\sin(\omega_k t)}{\omega_k},$$

$$\hat{f}_1(\omega)\hat{f}_2(\omega) \rightarrow \int_0^t f_1(t-\tau)f_2(\tau)d\tau.$$

Applying these two results enables us to invert

$$\frac{\hat{T}(\omega)}{\omega_k^2-\omega^2} \rightarrow \frac{1}{\omega_k}\int_0^t \sin(\omega_k(t-\tau))T(\tau)d\tau = T_k^n(t).$$

Plugging this time convolution into (18) yields

$$\begin{bmatrix} X^{(n)} \\ Y^{(n)} \end{bmatrix} = -\frac{L}{n\pi}R(x)T(t) + \frac{n\pi}{L}\sum_{k=1}^{2N+1} R_k^n T_k^n(t)|\psi_k^n> .$$

By recalling the definition of χ, the sine transformations and the half-range Fourier series for the eigenfunctions, we now can reconstruct the displacement components ξ_x and ξ_y as function of x, z and t

$$\xi_x(x,z,t) = \tag{20}$$
$$\frac{2}{L}\sum_{n=1}^{\infty}\sum_{m=1}^{N}\{\frac{n\pi}{L}\sum_{k=1}^{2N+1} R_k^n T_k^n(t)\alpha_{mk}^n\}\sin(m\pi x)\sin(\frac{n\pi}{L}z)$$
$$+R(x)T(t)\{1-\frac{z}{L}-\frac{2}{L}\sum_{n=1}^{\infty}\frac{L}{n\pi}\sin(\frac{n\pi}{L}z)\},$$
$$i\xi_y(x,z,t) = \tag{21}$$
$$\frac{2}{L}\sum_{n=1}^{\infty}\frac{n\pi}{L}\{\sum_{k=1}^{2N+1} R_k^n T_k^n(t)\frac{\beta_{0k}^n}{2}$$
$$+\sum_{m=1}^{N}(\sum_{k=1}^{2N+1} R_k^n T_k^n(t)\beta_{mk}^n)\cos(m\pi x)\}\sin(\frac{n\pi}{L}z),$$

where we omitted the trivial $e^{ik_y y}$ dependence. As a result of expression (9) the second term of (20) equals zero for all values of $z > 0$. However when $z = 0$ the second term equals $R(x)T(t)$ which is indeed the imposed footpoint motion.

Thus we have derived an analytical expression which describes the generation of linear MHD waves (coupled fast-Alfvén waves) by radially polarised footpoint motions. The solution is written as a superposition of eigenmodes $|\psi_k^n>$ whose excitation is determined by the time dependence $T(t)$ of the footpoint motion through the convolution T_k^n and by the spatial dependence $R(x)$ of the footpoint motion through the scalar product R_k^n. This expression can be easily evaluated numerically at any time with the structure of the waves being fully resolved as long as a sufficiently large numbers of sines in both x and z directions are taken into account.

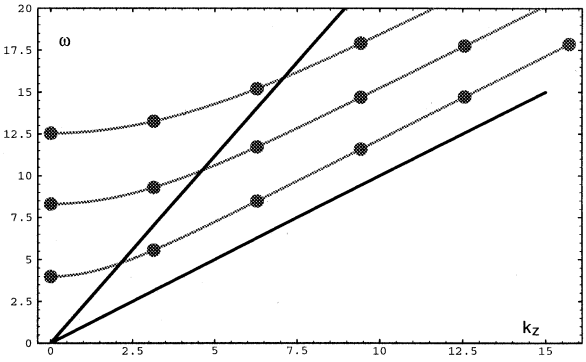

Fig. 1. The eigenfrequencies of the first three fast eigenmodes (gray lines) together with the upper and lower bound of the Alfvén continuum (black lines) as function of k_z. The dots represents the relevant fast waves for the instructive example in Sect. 4.

4. Temporal evolution of resonant absorption

In this section we use the solutions (20) and (21) to follow the time-evolution of the resonant absorption process, starting from the imposed footpoint motion, the subsequent excitation of the quasi-mode, its resonant coupling to localised Alfvén waves and the resulting small length scales. In each step of this process we try to illustrate typical behaviour in different circumstances and discuss the possible 'bottlenecks'. In the next section then we discuss whether the resulting diffusion time-scales are sufficiently short (in comparison with typical lifetimes of coronal loops) to contribute to coronal heating.

As an illuminating example (rather than a realistic model) we consider the system described in Sect. 2 with $\rho_A = 0.6$, $\rho_B = 0.4$ and $L = a = 1$ (in dimensionless units) corresponding to a range of Alfvén speeds of 1 (inside the loop) up to 2.24 (outside the loop) (all in dimensionless units) and we take k_y=1.

Before starting the simulation it turns out to be very instructive to look at the eigenfrequencies of the fast and Alfvén waves as function of k_z in the case that they are uncoupled ($k_y = 0$). Fig. 1 shows the eigenfrequencies of the first three fast eigenmodes together with the upper and lower bound of the Alfvén continuous spectrum as function of k_z. As seen from the expressions (20) and (21) which describe the solution as a superposition of eigenmodes, the possible values of k_z are multiples of π/L. The corresponding eigenfrequencies of the fast waves are indicated in Fig. 1 as dots. The different gray lines connect fast modes with the same number of nodes in the x-direction, with the lowest gray line connecting modes with zero nodes in the x-direction.

The fast modes corresponding to an eigenfrequency above the Alfvén continuum are travelling waves in the exterior coro-

nal environment. In an open system these 'leaky' modes would radiate their energy away from the loop. In our closed box model of a coronal loop they are artificially kept in the neighbourhood of the loop. The modes with frequency within the range of the continuous spectrum are evanescent in the exterior coronal environment and thus correspond to body modes of the loop itself. When $k_y \neq 0$ they couple to localised Alfvén waves and form so-called quasi-modes. Since these quasi-modes are evanescent outside the loop, their behaviour is not really influenced by the rigid wall condition at $x = 1$ and so our closed box is a reasonable model to study the quasi-mode behaviour. Tirry & Goossens (1996) presented an easy numerical scheme to calculate the complex frequencies of these quasi-modes. With this scheme we determined the oscillation frequency of the fundamental ($k_z = \pi/L$) quasi-mode to be $\omega = 5.551$ which corresponds to the local Alfvén frequency at $x = 0.746$.

4.1. The excitation of the quasi-mode by the footpoint motion

To illustrate the time-evolution of the perturbation due to a radially polarised footpoint motion, we evaluate expressions (20) and (21) with the following characteristics

$$R(x) = 0.01 \sin(\pi x),$$
$$T(t) = \begin{cases} \frac{1}{4}(\frac{t}{t_0})^2 e^{2-\frac{t}{t_0}} & \text{for} \quad t \leq 2t_0 \\ \cos(\omega_d(t-2t_0)) & \text{for} \quad t > 2t_0. \end{cases}$$

with $t_0 = 0.2$. The t^2-dependence in the initial phase of $T(t)$ is included to guarantee that the initial conditions (6) are trivially fulfilled. The subsequent harmonical driving with frequency ω_d might not be in accordance with the stochastic nature of the convective footpoint motions that one can expect in the photosphere, but we tried to keep the simulation as transparant as possible. In future work we plan to investigate time dependencies such as finite wave-packets, pulses or white noise.

The convergence of the series has been checked. Because the fast waves are reflected on the boundaries of the loop, fine structure in the z-direction corresponding to the so-called Pekeris-effect in the ξ_x component will develop as shown by Berghmans, De Bruyne & Goossens (1996). Therefore a large number of sines in the z-direction has to be taken into account in the expression (20) for ξ_x to converge in comparison with the number of sines in the expression (21) for ξ_y, corresponding in essence to the Alfvén waves which propagate along the magnetic field-lines.

In a first step we take $\omega_d = 3.551$ which is far from any quasi-mode frequency (see Fig. 1) but within the Alfvén continuous spectrum for $k_z = \pi/L$ and corresponding to the local Alfvén frequency at $x = 0.35$. The quantity $i\xi_y(x, z = 0.5L)$ is plotted in Fig. 2 for different times $t = 10, 20, 40$. In addition to a resonance, which is built up at the magnetic surface $x = 0.35$ where the local Alfvén frequency equals the driving frequency, there is also an energy transfer from the initially excited fundamental fast body wave towards the corresponding resonant Alfvén waves followed by a phase-mixing process around $x = 0.746$.

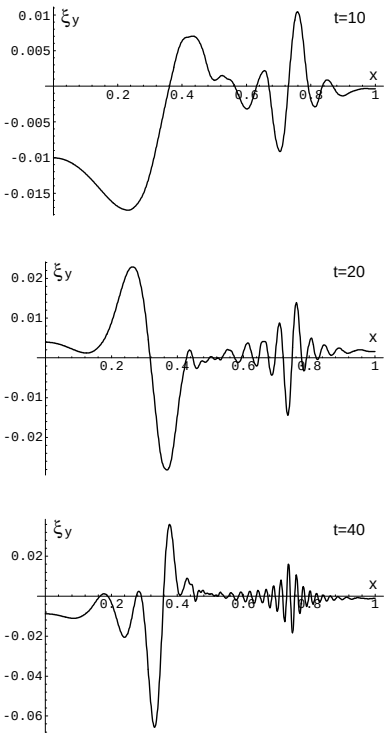

Fig. 2. The ξ_y component as function of x at the height $z = 0.5L$ for three different times $t = 10, 20, 40$ with the driving frequency $\omega_d = 3.551$ in the Alfvén continuum but away from any quasi-mode frequency.

In a next run we drive with the quasi-mode frequency $\omega_d = 5.551$ (see Fig. 3, 4). It is immediately clear that the resonance is much more pronounced both in amplitude and width. This is a consequence of two resonances. First, since we drive at the quasi-mode frequency, the footpoint frequency is matched to one of the natural global oscillation frequencies of the loop, namely the lowest quasi-mode frequency. This results in an enhanced excitation seen in the ξ_x component as shown in Fig. 3. Secondly, the Alfvén resonance induces a resonant coupling between the excited quasi-mode and the localised Alfvén waves as seen in ξ_y component in Fig. 4. Fig. 4 shows that the solution oscillates between a smoothed δ profile (see $t = 10$ and $t = 40$) and a $1/x$ profile ($t = 20$) which is to be expected for the Alfvén resonance (see e.g. Fig. 1 in Goossens & Ruderman 1995; Goossens, Ruderman & Hollweg 1995).

Let us now investigate how the spatial variation of the radially polarised footpoint motion is involved in the efficiency of the excitation of the global modes. This can be seen in the analytically derived expressions (20) and (21) which describe the solution in time as a superposition of eigenmodes whose excitation is determined by the time dependence of the footpoint motions through the convolution $T_k^n(t)$ and by the spatial dependence of the footpoint motions through the scalar product R_k^n. Since the spatial solutions of the fundamental fast eigenmode has no nodes (bottom gray line in Fig. 1), they are expected to be excited more efficiently by global footpoint motions without a node in its spatial dependence. This is shown in Fig. 5 where the amplitude of

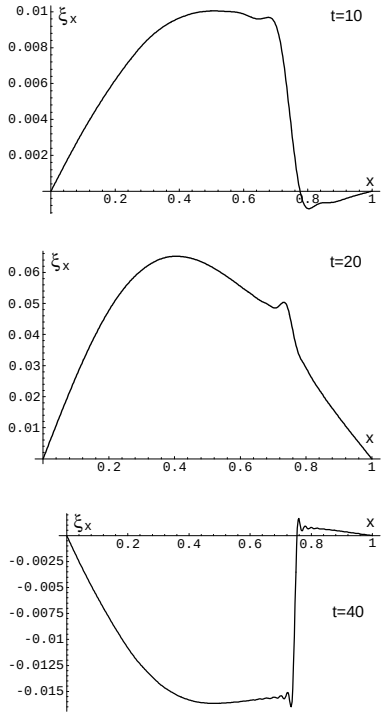

Fig. 3. The ξ_x component as function of x at the height $z = 0.5L$ for three different times $t = 10, 20, 40$ with the driving frequency equal to the first quasi-mode frequency $\omega_d = 5.551$.

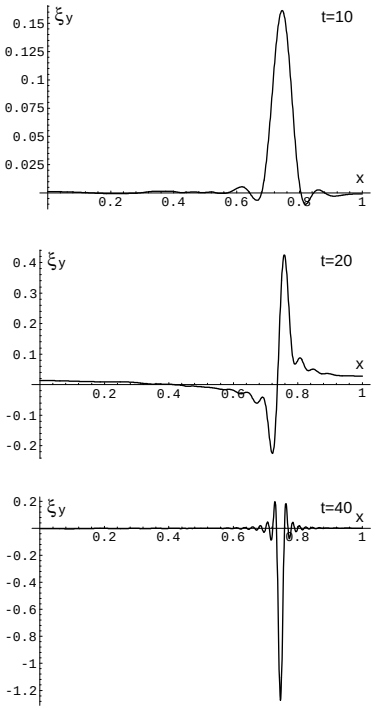

Fig. 4. The ξ_y component as function of x at the height $z = 0.5L$ for three different times $t = 10, 20, 40$ with the driving frequency equal to the first quasi-mode frequency $\omega_d = 5.551$.

$\xi_y(z = 0.5L)$ at the resonant position is plotted as function of time for $\omega_d = 5.551$ with $R(x) \sim \sin(\pi x), \sin(2\pi x), \sin(3\pi x)$.

4.2. The coupling of the quasi-mode to localised Alfvén waves

It was already mentioned in the introduction that the Eqs. (4) and (5) are decoupled when $k_y = 0$, and fast waves and Alfvén waves exist as independent modes. The restriction to $k_y = 0$ allowed many authors working on footpoint driven MHD waves to obtain a considerable simplification in their study, but in addition suppresses the Alfvénic resonance.

The value of the wave number k_y determines the strength of the coupling between the global mode and the corresponding resonant Alfvén wave. The wave number k_y thus acts as a coupling-parameter and its influence needs a closer examination. In Fig. 6 we show the shift of the eigenfrequencies of the fundamental fast waves corresponding to $k_z = \pi/L, 2\pi/L, 3\pi/L$ into the complex frequency plane when k_y is steadily increased from 0 to 1. The damping rate (ω_i) of the quasi-mode increases for k_y increasing from 0 to 1, whereas the oscillation frequency remains almost constant. Since $k_y = 1$ results in a faster damping of the quasi-mode by conversion to the resonant Alfvén waves than say, $k_y = 0.2$ we can expect that the growth of the Alfvén resonance will be slower in the last case. This influence on the growth of the resonance is indeed seen in Fig. 7 where the amplitude of $\xi_y(z = 0.5L)$ at the resonance point $x = 0.746$ is plotted as function of time.

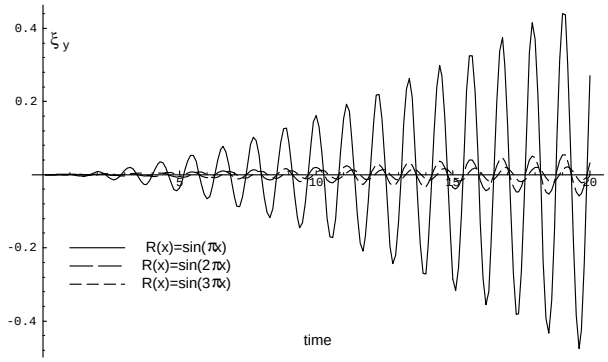

Fig. 5. The amplitude of ξ_y at the resonance as function of time with the driving frequency $\omega_d = 5.551$ with radial dependence of footpoint motion $R(x) \sim \sin(\pi x), \sin(2\pi x), \sin(3\pi x)$.

4.3. The decrease of length scales

Because of the extraordinary high Reynolds numbers in the solar corona, global plasma processes yield virtually no dissipation. In order to achieve the observed energy losses, extremely small length scales have to be generated. In this section we want to investigate how effective resonant absorption is in producing these small length scales. To do so we plot the length scale L_R of the resonance layer as function of the physical time (Fig. 8). The length scale of the resonance is defined as the full width at half of maximum height. L_R is plotted in Fig. 8 for the resonances corresponding to (A) $\omega_d = 3.551$ (off quasi-mode frequency)

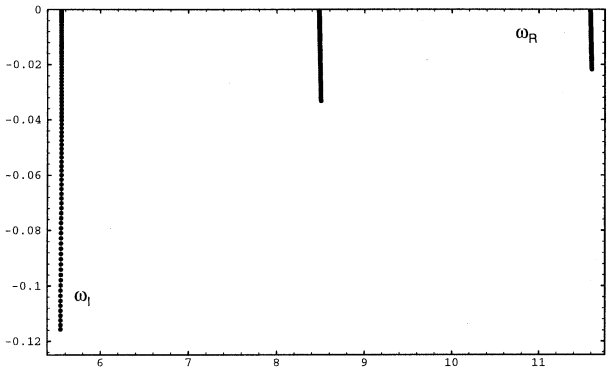

Fig. 6. The shift of the eigenfrequencies in the complex frequency plane of the three quasi-modes corresponding to $k_z = \pi/L, 2\pi/L, 3\pi/L$ when k_y is steadily increased from 0 to 1.

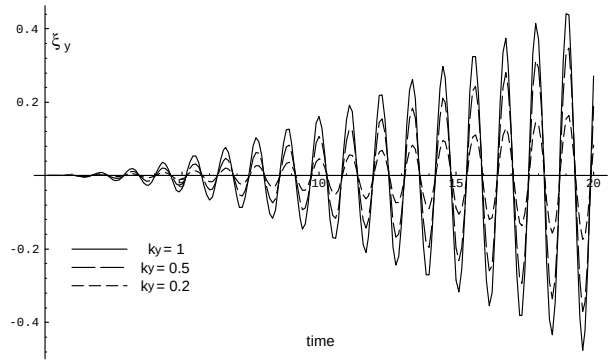

Fig. 7. The amplitude of ξ_y at the resonance as function of time for $k_y = 0.2, 0.5, 1$ with the driving frequency $\omega_d = 5.551$.

and (B) $\omega_d = 5.551$ (on quasi-mode frequency). The difference in reduction of the length scale is clear, but the length scales associated with the resonances in both cases decrease proportional to the inverse of time in agreement with the results of Mann, Wright & Cally (1995). We have also plotted the reduction in length scale of the resonance associated with the initially excited fundamental global mode in the case $\omega_d = 3.551$ (C). Due to the phase-mixing process the resonance length scale is substantially reduced, also proportional to the inverse of time. However, since the fundamental global mode is only initially excited, the amplitude corresponding to this resonance remains relatively small (see Fig. 2).

We also looked for the dependence on k_y of the generation of small length scales. In Fig. 9 we have plotted the length scale as a function of time for $k_y = 0.2, 0.5, 1$ and $\omega_d = 5.551$ (the oscillation frequency of the first global mode). It turns out that the length scale corresponding to the resonance is not appreciably influenced by the value of k_y as shown in Fig. 9 for $k_y = 0.2, 0.5, 1$ and $\omega_d = 5.551$ (the oscillation frequency of the first global mode).

Finally the influence of $R(x)$ on the developping length scales was investigated (Fig. 10) but again no significant influence was noted (except maybe in the initial phase).

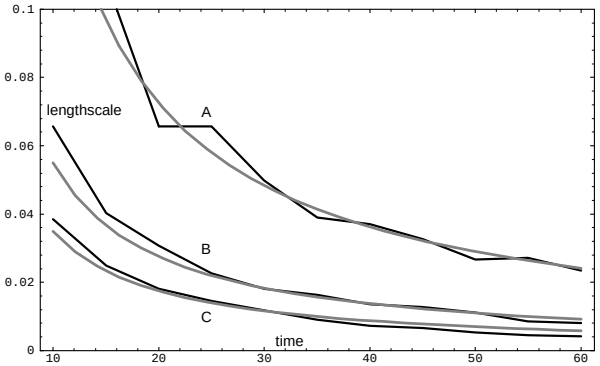

Fig. 8. The length scale of the resonance (defined as the full width at half of maximum height) as function of time. The length scale decreases proportional to the inverse of time. (A) corresponds to the resonance when $\omega_d = 3.551$, (B) to the resonance when $\omega_d = 5.551$ (quasi-mode frequency), (C) to the resonance associated with the initially excited first global mode when $\omega_d = 3.551$.

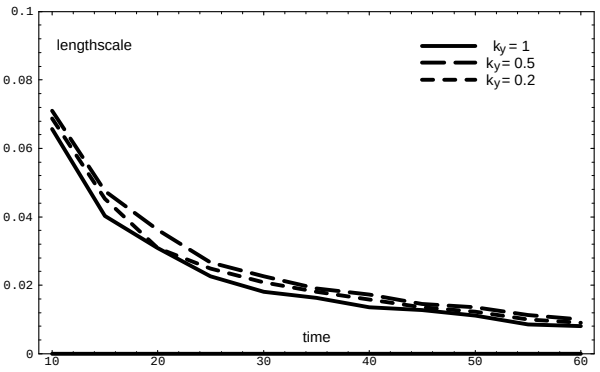

Fig. 9. The reduction of the length scale of the resonance in time with driving frequency $\omega_d = 5.551$ (quasi-mode frequency) for $k_y = 1, 0.5, 0.2$.

In the next section more realistic loops with different aspect ratios will be considered in order to investigate the dissipation time scales corresponding to the smallest but important length scale that can be achieved by the radially polarised footpoint motions during an acceptable lifetime of a coronal loop.

5. Diffusion time-scales

For resonant absorption to be a viable heating mechanism for coronal loops the generation of small scale dissipative features should at least take place on time scales shorter than the lifetime of coronal loops. These time scales can be estimated from our ideal temporal simulations by expressing the dissipation time scale (function of the resonance length scale) as function of the physical time. Another requirement is that the resonant absorption of Alfvén waves provides the observed volumetric heating rates in coronal loops. The averaged observed energy fluxes are approximately $3 \times 10^2 W/m^2$ in the quiet corona up to $10^4 W/m^2$ in the active region loops (Hollweg 1990).
Imaging data from high resolution Normal-Incidence X-ray

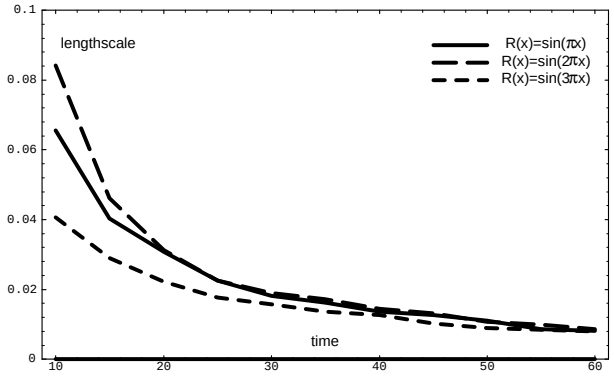

Fig. 10. The reduction of the length scale of the resonance in time with driving frequency ω_d = 5.551 (quasi-mode frequency) for radial dependence of the footpoint motion $R(x) \sim \sin(\pi x), \sin(2\pi x), \sin(3\pi x)$.

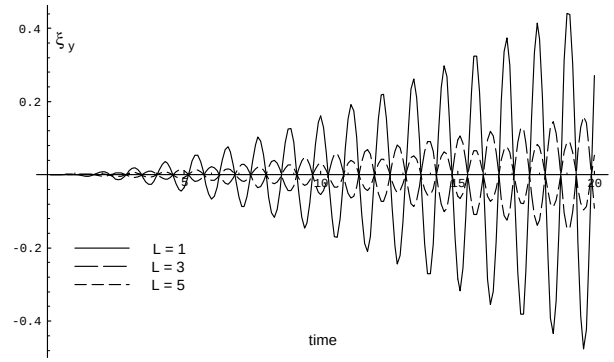

Fig. 11. The amplitude of ξ_y at the resonance as function of time with the driving frequency ω_d = 5.551 (quasi-mode frequency) for loop length $L = 1, 3, 5$.

Telescope (NIXT) observations (Golub et al., 1990) reveal coronal loop dimensions in the ranges

$$2 \times 10^7 \mathrm{m} \leq\ L\ \leq 2 \times 10^8 \mathrm{m}$$
$$4 \times 10^5 \mathrm{m} \leq\ a\ \leq 4 \times 10^6 \mathrm{m}$$

A typical Alfvén speed in the solar corona is of the order of 10^6m/s so that the Alfvén transit time along the loop varies, let say, from 5 to 100 seconds. Fig. 11 shows the amplitude of ξ_y at the resonance position for $L = 1, 3, 5$ (corresponding to Alfvén transit times of $1, 3, 5$) and for the driving frequency equal to the quasi-mode frequency ω_d = 5.551. It can be clearly seen that the longer the loop is the slower the resonance amplitude increases, since for larger Alfvén transit times it takes longer for the resonantly excited Alfvén waves to interfere constructively. The amplitude at the resonance scales proportional to the inverse of the loop length. In Fig. 12 the length scale of the resonance is plotted as function of time for $L = 1, 3, 5$ with the driving frequency ω_d = 5.551. The decrease of the length scale by the resonant absorption in time seems to be independent of the length of the loop. Hence once the global mode is excited, the length of the loop is not involved in the generation of small scales in the radial direction by the resonant absorption of Alfvén waves, but of course it will be important for the

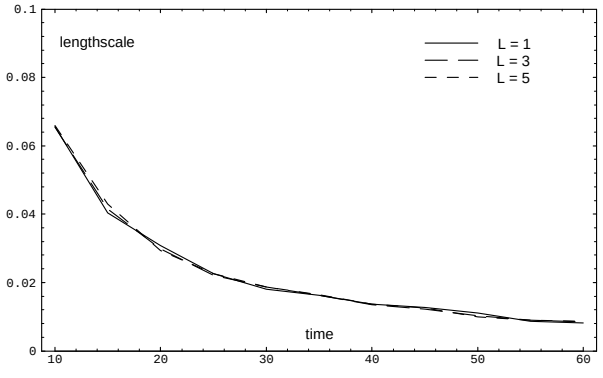

Fig. 12. The reduction of the length scale of the resonance in time with driving frequency ω_d = 5.551 (quasi-mode frequency) for loop length $L = 1, 3, 5$.

volumetric heating rate. This result allows us to investigate the reduction of the length scale corresponding to the resonance with small values of L which saves a lot of CPU time.

In plasmas, the diffusion time scales depend on the typical length scale. We will use the resistive diffusion time scale τ_{diff} to estimate the time when dissipation becomes important and thus our ideal MHD simulations stop to be valid. The resistive diffusion time scale is estimated as l^2/η, where l denotes a typical length scale and η denotes the magnetic diffusivity. For the solar coronal conditions, the magnetic diffusivity η is of the order of $1m^2/s$ (Priest, 1987) so that $\tau_{diff} \sim l^2$. Typical life times of coronal loops varies from 6 to 24 hours. For dissipation to become important the dissipation time scale should be reduced less than the half of the life time of the coronal loop. This means that length scales about 100 meter should be generated within half of the life time of the coronal loop. The length scales in the ξ_y component produced by resonant absorption reduce proportional to the inverse of time (Mann, Wright & Cally 1995). Using the fit $l = 0.6 \times 10^6/t$ (Fig. 8 (B)), the time needed to generate a length scale about 100 meter lies between 2 and 3 hours. So dissipation seems to become important in a time of the order of the life time of the loop. This is a rather rough estimation, but certainly not an overestimation in linear theory. Hence at first sight it looks as if that the necessary small scale dissipative features are created sufficiently fast, resulting in a substantial heating of the coronal loop. Numerical nonlinear simulations by Ofman & Davila (1995) show that the highly sheared velocities at the narrow resonance layer are subject to a Kelvin-Helmholtz like instability. They also found that the resonant absorption heating layers are not destroyed by the Kelvin-Helmholtz instability. This instability may lead to turbulent enhancement of the dissipation parameters and acceleration to smaller length scales (Hollweg & Yang 1988) and account for the observed turbulent velocities inferred from the nonthermal broadening of X-ray and EUV emission lines.

Hence it seems fair to conclude that the resonant absorption of Alfvén waves indirectly excited by radially polarised footpoint motions through a global mode generates the small length scales necessary for coronal heating in time.

6. Conclusions and discussion

The main object of this paper was to give an answer to the question whether resonant absorption of Alfvén waves indirectly driven by radially polarised footpoint motions through a global mode generates the necessary small scale dissipative features consistent with the dissipation coefficients corresponding to coronal conditions and the usually assumed length scales and life times for coronal loops. We modelled a coronal loop as a straight, static plasma slab, obeying the set of ideal MHD equations in the zero-β-approximation. In this approximation we were able to write the general solution for the temporal evolution of the excited linear MHD waves as a superposition of eigenmodes (representing coupled Alfvén-fast waves) where the time dependence of the footpoint motion enters in the expressions through convolutions and the radial dependence of the footpoint motion through scalar products. The analytically derived solution can be easily evaluated numerically at any time with the structure of the waves being fully resolved as long as a sufficient number of sines in both the x and z direction are taken into account.

By considering an instructive example, the importance of the global modes on the resonant absorption of energy was demonstrated. Since the radially polarised footpoint motion, which is certainly present in the velocity field described by the convective motions, does not excite the torsional Alfvén waves directly, an intermediate mode is necessary to transfer efficiently the energy to the Alfvén resonance, what is exactly done by the quasi-mode. The spatial variation of the radially polarised footpoint motions determines the efficiency of the excitation of the global modes whereas the strength of coupling between the global modes and the corresponding resonant Alfvén waves is determined in essence by the wave number k_y.

It is shown that the length scales of the resonance reduces proportional to the inverse of time as it does in the case of sideways excitation. The length of the loop does not have an influence on this time evolution of the resonance length scale. Once the global mode is excited in the whole of the loop, the length of the loop is not involved in the development of small scales in the radial direction by coupling to the corresponding resonant Alfvén wave. However it is important to note that the longer the loop, the smaller the possible values of k_z and the difference between the possible k_z are, hence the more global modes with relatively low frequencies exist.

Although the simulations are carried in ideal MHD, by following the dissipation time scale (corresponding to the resonance length scale) as function of the physical time, a time when dissipation would start to become important, can be estimated. With a rather rough estimation, but certainly not an overestimation, we came to the conclusion that in linear MHD dissipation becomes important in a time scale comparable to the life time of the coronal loops.

So if the Kelvin-Helmholtz instability due to the highly sheared velocities at the narrow resonance layer leads to turbulent enhancement of the dissipation parameters and an acceleration to smaller length scales (Hollweg & Yang 1988; Ofman & Davila 1995), we can state that resonant excitation of Alfvén waves through a global mode by radially polarised footpoint motions develops small enough dissipative features in acceptable time scales. There could also exist some anomalous processes which raise the effective values of the dissipation coefficients, but they should then be identified.

Probably one of the most challenging problems concerning the wave heating theory as an explanation for the heating of coronal loops is whether the convective bulk motions offer the sufficient power at the right frequency ranges, which are relatively high compared to the turn over time of the individual granules.

It also remains to be demonstrated that the necessary volumetric heating rate by resonant absorption can be accomplished with velocity oscillations similar to those which are observed.

Acknowledgements. The authors greatfully acknowledge the valuable discussions with P. De Bruyne and M. Ruderman.

References

Berghmans, D., & De Bruyne, P. 1995, ApJ, 453, 495
Berghmans, D., De Bruyne, P., & Goossens, M. 1996, ApJ, november
Cally, P.S. 1991, J. Plasma Phys., 45, 453
Cheng, C.C., Doschek, G.A., & Feldman, U. 1979, ApJ, 227, 1037
Goedbloed, J.P. & Halberstadt, G. 1994, A&A, 286, 275
Goedbloed, J.P. 1994, International Conference on Plasma Physics, in press
Golub, L., Herant, M., Kalata, K., Louas, I., Nystrom, G., Pardo, F., Spiller, E., & Wilczynski, J. 1990, Nat, 344, 842
Goossens, M., Ruderman, M.S., & Hollweg, J.V. 1995, SPh, 157, 75
Goossens, M., & Ruderman, M.S., 1995, Physica Scripta, Vol T60, 171
Halberstadt, G., & Goedbloed, J.P. 1993, A&A, 280, 647
Halberstadt, G., & Goedbloed, J.P. 1995, A&A, 301, 559
Halberstadt, G., & Goedbloed, J.P. 1995, A&A, 301, 577
Hollweg, J.V. 1984, ApJ, 277, 392
Hollweg, J.V., & Yang, G. 1988, J. Geophys. Res., 93, 5423
Hollweg, J.V. 1990, Comp. Phys. Rep., 12, 205
Mann, I.R., Wright, A.N., & Cally, P.S. 1995, J. Geophys. Res., 100, 19441
Ofman, L., & Davila, J.M. 1995, J. Geophys. Res., 100, 23427
Ofman, L., & Davila, J.M. 1996, Astrophys. Lett., 456, L123
Parker, E.N. 1972, ApJ, 174, 499
Parker, E.N. 1992, J. Geophys. Res., 97, 4311
Poedts, S., Goossens, M., & Kerner, W. 1989, Solar Phys., 123, 83
Poedts, S., & Kerner, W. 1991, Phys. Rev. Lett., 66, 22
Poedts, S., & Kerner, W. 1992, J. Plasma Phys., 47(1), 139
Poedts, S., Beliën, A.J.C., & Goedbloed, J.P. 1994, Solar Phys., 151, 271
Poedts, S., & Boynton, G.C. 1996, A&A, 306, 610
Priest, E.R. 1987, Solar Magnetohydrodynamics, D. Reidel Publishing
Ruderman, M.S., Berghmans, D., Goossens, M., & Poedts, S. 1996, A&A, accepted
Saba, J.L.R., & Strong, K.T. 1991, ApJ, 375, 789
Steinolfson, R.S., & Davila, J.M. 1993, ApJ, 415, 354
Tirry, W.J., & Goossens, M. 1996, ApJ, 471, 501
Ulrich, R.K. 1996, ApJ, accepted
Van Ballegooijen, A.A. 1985, ApJ, 298, 421
Wright, A.N., & Rickard, G.J. 1995, ApJ, 444, 458
Zirker, J.B. 1993, Solar Phys., 148, 43